Hydrogen skeleton, mobility and protein architecture

Kalman Tompa[1], Monika Bokor[1], Kyou-Hoon Han[2,3] and Peter Tompa*[4,5]

[1]Institute for Solid State Physics and Optics; Wigner RCP of the HAS; Budapest, Hungary; [2]Department of Bioinformatics; University of Science and Technology; Yuseong-gu, Korea; [3]Biomedical Translational Research Center; Division of Convergent Biomedical Research; Korea Research Institute of Bioscience and Biotechnology; Yuseong-gu, Korea; [4]Institute of Enzimology; Research Centre for Natural Sciences of the HAS; Budapest, Hungary; [5]VIB Department of Structural Biology; Vrije Universiteit Brussel; Brussels, Belgium

The mobility of the proton-proton radial vectors is introduced as a quantitative measure for the structural dynamics of organic materials, especially protein molecules. As defined for the entire molecule, the hydrogen mobility (*HM*) is proposed as an "order parameter", which describes the effect of motional narrowing on inter-proton dipole-dipole interactions. *HM* satisfies all requirements of an order parameter in the Landau molecular field theory of phase transitions. The wide-line NMR second moments needed to obtain *HM* are exactly defined and measurable physical quantities, which are not produced by mathematical fitting and do not carry the limitations and restrictions of any model (theoretical formalism). We first demonstrate the usefulness of *HM* on small organic molecules with data taken form the literature. We outline its link with structural and functional characteristics on a range of proteins: *HM* provides a model-free parameter based on first principles that can clearly distinguish between globular and intrinsically disordered proteins, and can also provide insight into the behavior of disease-related mutants.

Introduction

The importance of the dynamic nature of protein molecules cannot be overestimated: understanding their function in its entirety cannot be achieved by considering them as rigid molecules. Their dynamic state is affected by their thermal and chemical surroundings. The limitations of information inherent in the applied experimental method(s) also cannot be neglected. Beyond the general and conceptual question of motion (to the effect as it is detailed in Appendix A), the identification and proportion of mobile parts (residues), the physical characteristics of their motion and the effect of mobility on their reactivity/function all require special attention.

Addressing mobility is motivated by works approaching this subject from different angles. Halle criticized experimental approaches and results on aqueous protein solutions, by stating that "the progress is less and erratic and the results given by different experimental methods are contradictory and more or less model dependent in the interpretation"[1]. Saito and Kobayashi examined carefully the physical basis of protein architecture.[2] Wlodawer and colleagues discussed the limitations of structural information obtained by X-ray crystallography.[3] They emphasized the lack of direct determination of hydrogen positions, which suggests the role of proton magnetic resonance experiments to complement such measurements very effectively. The

regular and generally used NMR procedures were summarized e.g., by Dyson and Wright, with particular focus on intrinsically disordered proteins,[4] by Duer in the case of studying molecular motions in solids,[5] by Antzutkin in molecular structure determination in biology,[6] and by Smith in the case of studying protein structures.[7] The change in protein structural paradigm from order to disorder (from globular to intrinsically disordered (ID) proteins) was discussed in reference 8. Realizing the limitations of all approaches applied to date, we would like to add a novel wide-line NMR approach to complement the usual set of methods; the experimental analyses (including wide-line NMR) of the IDPs were introduced earlier in references 9 and 10.

Our experimental approach relies on wide-line NMR spectrometry, as we seek global, non-selective information. The elementary probe we use is the atomic nucleus of hydrogen (the proton magnetic dipolar moment) residing in the protein molecules. The relevant variants of wide-line NMR spectrometry are detailed in the book chapters 12 in reference 9, and 13 in reference 10. The wide-line spectrum and its even moments, especially the second moment (a main indicator of internal motion in solids; see Appendix B) are used here as a first step. In prior works, we outlined the physical basis of the applied method and detailed the evaluation and interpretation protocols. The key factor in our approach is the hydrogen mobility (i.e., the time dependence of proton-proton radial vectors), which is indicative

of NMR-visible motions and not the high-frequency lattice vibrations. This hydrogen mobility introduced depends on the molecular structure, temperature, and also on the chemical environment in the case of solutions.

In the paper, we describe in detail the theoretical basis of the second moment of the NMR spectrum. We first consider the case of a rigid lattice; the motional narrowing is treated subsequently. We give the definition of the novel order parameter we term hydrogen mobility, and put it into the context of order parameters in general. We then review the experimental second moment data found in the literature for several organic compounds and we calculate the corresponding hydrogen mobility values. We test and give reasons for the application of hydrogen mobility. Based on experimental data, we calculate the hydrogen mobility factors for some selected proteins, and discuss the importance of hydrogen mobility as a global, model-free order parameter in describing function-related features of flexibility of proteins.

NMR Spectrum, Even Moments, and Multi-Component Wide-Line Spectrum of "Solids"

Rigid lattice

This section is prefaced with the remark that there is no analytical description of the spectra of multi-spin systems (e.g., molecules made of numerous atomic nuclei of various types). The series expansion technique can be used[11,12] to obtain a moments expansion of the time-domain NMR-signal (FID or solid echo).

The magnetic dipolar interaction plays a key role in the wide-line spectroscopy of solids. The magnitudes (or lengths) of the vectors connecting the interacting nuclei and their directions with respect to the external magnetic field directly determine the architecture (geometrical arrangement, structure or topology) of the nuclear spin system. This is the reason why the direct measurement of dipolar interactions is essential for describing the structure of proteins. The basic quantum theory of the dipolar interaction and properties of the NMR spectrum was given by Van Vleck in his Nobel laureate work.[13] Determining the second moments is viewed as a first step, used subsequently to characterize the rigid lattice and the internal motions of molecules.

To understand the NMR characteristics, the wide-line NMR spectrum and the even moments, and to lay the groundwork for planning and interpreting the experiments, we invoke short parts from Abragam's (chapters IV and X, ref. 14) and Slichter's (chapter 13, ref. 15) basic monographs.

On the basis of the Van Vleck theory, the second moment coming from dipole-dipole interaction between identical spins (II) is (p. 79, ref. 15)

$$\left\langle \Delta B^2 \right\rangle_{II} = \frac{3}{4}\gamma^2\left(\frac{\hbar\mu_0}{4\pi}\right)^2 I(I+1)\frac{1}{N}\sum_{j,k}\frac{\left(1-3\cos^2\theta_{jk}\right)^2}{r_{jk}^6} \qquad (1)$$

where γ is the gyromagnetic ratio, μ_0 is the magnetic constant, N is the number of nuclei, r_{jk} is the magnitude of the vector connecting the ith and j^{th} nuclei, θ_{jk} is the angle between the

internuclear vector $\mathbf{r}_{jk}$ and the time independent magnetic induction vector $\mathbf{B}_0$, and the double summation means averaging over all the spins and all the neighbors. If all the resonant spins are located in equivalent positions, the double summation is reduced to a single one, being independent from one of the indices. There are then N equivalent sums, one for each value of j. The second moment is

$$\left\langle \Delta B^2 \right\rangle_{II} = \frac{3}{4}\gamma^2\left(\frac{\hbar\mu_0}{4\pi}\right)^2 I(I+1)\frac{1}{N}\sum_{k}\frac{\left(1-3\cos^2\theta_{jk}\right)^2}{r_{jk}^6} \qquad (2)$$

in that case. (We have to emphasize that it is not the case with protons in proteins, in spite of the general claim in some papers.) Each term in Eqs. 1 and 2 is clearly of the order of $\left(B_{\text{loc}}^k\right)^2$, where B_{loc}^k is the contribution of the kth spin to the local field at spin j. Equations 1 and 2 precisely define the local field, which enables one to compare an exactly defined theoretical quantity with the measured (experimental) value. The summation has a short range character because of the strong distance dependence of the r_{jk}^{-6} term.

It is also necessary to address what "equivalent positions" mean in general and especially in a protein molecule? "The equivalent arrangements of the non-zero nuclear magnets around the resonant nuclei" gives the answer. In our case, not all the protons are equivalent, and consequently, a few terms from one part of the double summation are to be used in the second moment calculation. How many? Decomposition of the components in the wide-line spectrum helps to estimate the number.

If, besides protons, there are also other nuclear species, they also contribute to the local fields and to the total second moment (the contribution is given in ref. 15 not necessary for us at this moment). In the case of proton resonance, the dipolar contributions of other nuclei (e.g., ^{13}C, ^{15}N, ^{17}O) are zero or negligible; this is not true for other species (e.g., ^{23}Na or ^{35}Cl).

As a consequence, the hydrogen nuclei (the protons) give the topological map of the immobile protein molecule and the rigid protein-water system (which we may term the hydrogen skeleton). The use of Eq. 1 or Eq. 2 gives the theoretical basis for controlling the topological construction of the hydrogen skeleton of our molecules. It is to be mentioned, again, that the arrangement of the hydrogen atoms is missing from the X-ray maps.[3]

Both the length and direction of the $\mathbf{r}_{jk}$ proton-proton vectors are given as structural elements in single crystals. Only the length of the proton-proton vector exists in a powder (polycrystalline or lyophilized) sample because of "space-averaging". The second moment then simply depends on the length (magnitude) of $\mathbf{r}_{jk}$. For interacting spin-pairs, the contribution to the second moment of the rigid lattice is

$$\left\langle \Delta B^2 \right\rangle_{RL} \propto \overline{\left(1-3\cos^2\theta_{jk}\right)^2} \qquad (3)$$

The fourth moment is only used here as a control for the analytical form of the line shape in Chapter 4 (wide-line NMR spectra and second moments of proteins), i.e., the details are not cited, only the references 10, 12, and 13 are mentioned again. The important point for our treatment is that the ratio of the

fourth moment to the second moment-square is 3 for a Gaussian line.

Motional narrowing

Observing the temperature dependence of the systems studied, the position of protons and the dipole-dipole interaction between the neighboring pairs will be time dependent. The second moments (Eqs. 1 and 2) will be time dependent by the r_{jk} and θ_{jk} quantities as a consequence of atomic motions. The phenomenon is known as motional narrowing[11,12] and the results are the narrowing of the NMR spectrum and reduced moments as a consequence of time averaging. For a spin pair, Abragam[14] and Slichter[15] following Andrew and Eades[16] gave the description of time averaging by rotation around a given axis

$$\left\langle \Delta B^2 \right\rangle_{\text{rot}} = \left\langle \Delta B^2 \right\rangle_{\text{RL}} \left(\frac{3\cos^2 \gamma_{jk} - 1}{2} \right)^2 \qquad (4)$$

where γ_{jk} is the angle between the radius vector $\mathbf{r}_{jk}$ and the rotation axis. (If $\gamma_{jk} = 90°$, the time-averaged reduced moment is the rigid-lattice value reduced by the factor of 4.) Equation 4 forms the basis of the magic-angle spinning (MAS) method,[17] in which the sample is spun physically at the angle $\gamma_{jk} = 54°44'$ ($\cos^2\gamma_{jk} = 1/3$) with respect to the direction of the magnetic field. This way, the reduced second moment takes zero value for each spin pair. When there are internal molecular motions, the averaging is done also over the possible γ_{jk} angles, which does not result in zero value. The very simple reduction factor in Equation 4 is only valid for the intramolecular contribution to the second moment. The intermolecular contribution that results from interactions between spins that belong to different molecules is affected by the rotation in a more complicated way since both the distances between spins and the orientations of the spin-spin vectors change.

The two types of averaging, space-average and time-average, can be done for every topological and motional model. The summations (Eqs. 1–2) and several possible motions should be considered, not forgetting that the summation means that the individual contributions are added up. This procedure involves numerous assumptions about the topology and the motional states and, consequently, the results are model dependent. Instead, we chose to determine the second moments experimentally: both the reduced second moment and the rigid-lattice value can be measured. In the typical temperature-dependence of the NMR second moment, i.e., on the frequency of the internal motion, the decrease of the second moment occurs in a temperature range, the position and width of which depends on the material studied.[18]

Order parameter

An order parameter, which is characteristic of the motional state of the proton-proton pair, can be theoretically defined on the basis of Equations 1–4. This Hydrogen-Motional order parameter we intend to introduce, can be calculated by introducing the notation $\left\langle \Delta B^2 \right\rangle_{II} = M_2$ as

$$HM(T) = \frac{M_2(\text{RL}) - M_2(T)}{M_2(\text{RL})} \qquad (5)$$

Table 1. Second moments and hydrogen mobility for benzene and its deuterated versions.

Temperature	Motional state	M_2 [10^{-8} T^2]	HM
C_6H_6			
$T < 68$ K	Rigid lattice	9.72	**0**
145 K $< T <$ 230 K	Rotation around C axis	1.61	**0.83**
C_6H_5D			
$T < 68$ K	Rigid lattice	7.94	**0**
145 K $< T <$ 230 K	Rotation around C axis	1.86	**0.85**
1,3,5-$C_6H_3D_3$			
$T < 68$ K	Rigid lattice	3.57	**0**
145 K $< T <$ 230 K	Rotation around C axis	0.44	**0.88**

where $M_2(T)$ is the second moment measured at an arbitrary temperature T, $M_2(\text{RL})$ is the second moment measured in the rigid-lattice state at a sufficiently low temperature, and HM refers to the average mobility of the proton-proton vectors according to Equations 1–4. If the spectrum can be decomposed into e.g., two components as found in several cases, then two order parameters, i.e., two mobility values, can be measured. Equation 5 then takes the form

$$HM^x(T) = \frac{M_2(\text{RL}) - M_2^x(T)}{M_2(\text{RL})} \qquad (6)$$

where x = t, b, n means the "total," "broad," and "narrow" spectral components, respectively. HM^x is zero for an immobile (rigid/ordered) system and it is one for highly mobile (fluid-like) systems. The former state is probably realized at the temperature of liquid helium, whereas the latter one is only achieved above the melting point. There are two important points to be addressed: (1) What is the quantity to normalize with, i.e., what is the second moment of the rigid-lattice? (2) Which spectral component can be assigned to which part of the molecule?

"Order" is connected with the time dependence or mobility of the proton spin (nuclear magnetic moment) as $HM = 0$ for a rigid system and $HM = 1$ for the liquid state; both these states and intermediate states can also be measured. In Appendix C, some considerations are given for the "order parameters" as defined through the Lipari-Szabo formalism of protein-solvent systems.

About order parameters in general

We have learned from the thermal properties of solids, e.g., in reference 19 and especially in the Landau mean-field theory of phase transition[20] that a large variety of systems can be described by a single, temperature-dependent order parameter. The system might be the magnetization in ferromagnets, the dielectric polarization in a ferroelectric system, the fraction of superconducting electron-pairs in a superconductor, the director distribution in nematic liquid crystals,[21] or the fraction of neighbor A-B bonds of the total bonds in an alloy AB or A_3B. The physical quantity, which the order parameter refers to, is clearly given and its value must be between 0 and 1. The proposed $HM(T)$ satisfies these criteria.

Table 2. Second moments and hydrogen mobility for 1,4-dicyclohexylcyclohexane, cyclohexane and adamantane.

Temperature	Motional state	M_2 [10^{-8} T^2]	HM
1,4-dicyclohexylcyclohexane			
$T < 310$ K	Rigid lattice	24.9	**0**
335 K $< T <$ 344 K	Torsional oscillation	15.9	**0.36**
$T > 344$ K	Rotation around long axis	6.8	**0.73**
cyclohexane			
$T < 150$ K	Rigid lattice	26.5	**0**
156 K $< T <$ 186 K	Rotation around C axis	6.4	**0.76**
$T > 186$ K	Isotropic rotation	1.4	**0.95**
$T > {\sim}200$ K	Isotropic rotation + translational diffusion	~0	**~1**
adamantane			
$T \sim 4$ K	Rigid lattice	24.8	**0**
room temperature	Isotropic rotation	0.9	**0.95**

Experimental Second Moment Data in the Literature and Estimated Hydrogen Mobility

To appreciate the insight and relevance of *HM* as an order parameter in describing proteins, first we look into relevant data in the literature on small organic compounds. These results are related to motions of small molecules and parts of molecules, which helps us familiarize ourselves with the relevant orders of magnitude. The *HM(T)* values were calculated for cases where the second moment values were given at two temperatures at least.

The second moment measured for samples containing water of crystallization is $M_2 \sim 28 \cdot 10^{-8}$ T^2.[22] The expected second moment for H$\cdots$OH groups is only $M_2 \sim 3 \cdot 10^{-8}$ T^2.[23,24]

Works on the molecular motions detected in solid hydrocarbons[25-27] indicate the possible form of molecular motions, which range from torsional and rotational motions to translational diffusion. The second moment values measured for long-chain paraffins (n-C$_n$H$_{2n+2}$) at $T = 82$–99 K can be considered as rigid-lattice values with M_2 values given in **Table 1**;[25] these relevant spectra showed no fine structure. If the structure of a crystal is known and the lattice can be assumed rigid, the second moment of the proton resonance line can be calculated by applying the Van Vleck formula (Eq. 1). The crystal structure of n-C$_{29}$H$_{60}$ was given among the results of X-ray investigations of a series of normal paraffins (n-C$_i$H$_{2i+2}$; $i = 6 - 44$).[28-30] Although X-ray diffraction cannot give the locations of the hydrogen atoms, it accurately measures the C-C bond lengths. The geometric positions of the hydrogen atoms (protons) were then determined by assuming tetrahedral symmetry for the C-H bonds and by using the spectroscopic C-H bond lengths. The long-chain paraffins n-octadecane (n-C$_{18}$H$_{36}$), n-octacosane (n-C$_{28}$H$_{58}$) and dicetyl (n-C$_{32}$H$_{66}$) were investigated by continuous-wave NMR-spectroscopy.[25] These molecules consist of methylene and methyl groups. The rigid-lattice second moments measured at 82–99 K are $23.9 \cdot 10^{-8}$ T^2 ($i = 18$), $26.6 \cdot 10^{-8}$ T^2 ($i = 28$), and $27.1 \cdot 10^{-8}$ T^2 ($i = 32$). Fine structure in the spectra at that temperature was not found. On the basis of the Van Vleck theory and Equation 1, the theoretical M_2 values obtained are

$27.3 \cdot 10^{-8}$ T^2 ($i = 18$), $27.0 \cdot 10^{-8}$ T^2 ($i = 28$), and $26.9 \cdot 10^{-8}$ T^2 ($i = 32$).[25] The good agreement between the values measured and the ones calculated for n-octacosane and dicetyl proves the rigidity of the H skeleton, whereas the difference in the case of n-octadecane points to a small hydrogen mobility. The deviation from the two other paraffins is not surprising, because the lower melting point of n-octadecane also shows a looser crystal structure. The value of the *HM* mobility "order parameter" introduced here is 0.12.

Systematic investigations were done on benzene, by replacing H atoms partly with D (deuteron). The H-D change dilutes the magnetization of the H lattice, because of the much smaller nuclear moment of D, due to which its contribution to the second moment is approximately 2% of the proton magnetization. The great *HM* value (**Table 1**) can be explained by the rotation around the hexad axis of the full proton system (H-skeleton), that is, by the rotation of the benzene molecule. *HM* is practically independent of the H/D ratio.

In the case of N,N-dimethylanilin,[31] the connection of the –N(CH$_3$)$_2$ group to the benzene ring gives an estimated rigid lattice value of $M_2 = 18.4 \cdot 10^{-8}$ T^2. The measured second moment is $M_2 = 9.4\ldots 8.5 \cdot 10^{-8}$ T^2 in the temperature range of -190°C to 0°C, and it slowly decreases with increasing temperature, because of the lattice dilatation. The *HM* = 0.51 value is the consequence of the decrease of symmetry as compared that of the benzene. The actual value can be interpreted by the rotation of –CH$_3$ groups and by the immobility of benzene ring.

For urea,[32] the measured second moment is $M_2 = 20.8 \cdot 10^{-8}$ T^2 at ~195 K and it is $M_2 = 6.9 \cdot 10^{-8}$ T^2 at room temperature, and the hydrogen mobility estimated by us is *HM* = 0.87. The high value exhibits a molecular motion of high degree of symmetry, higher than that of the –NH$_2$ groups. Xylenes and mesitylene[33] give measured second moments of $9.8 \cdot 10^{-8}$ T^2 to $9.9 \cdot 10^{-8}$ T^2 at 95 K, which decrease upon heating to 205 K due to the lattice dilatation. The interpretation of the results is similar to that of the N,N-dimethylanilin, that is, rotation of methyl groups and the immobile benzene ring.

The experimental work on hexamethylbenzene[34] is outstanding regarding that several NMR characteristics were measured between 2 K and 450 K. The solid-echo radiofrequency pulse combination was used for the second moment measurements. The X-ray structure is known and the calculated rigid lattice second moment is $M_2 = 32.7 \cdot 10^{-8}$ T^2. The measured second moments are $20 \cdot 10^{-8}$ T^2 to $14.5 \cdot 10^{-8}$ T^2 in the 2 K to 50 K range, they take the values of $M_2 = 13.0 \cdot 10^{-8}$ T^2 at 90 K, and $M_2 = 2.5 \cdot 10^{-8}$ T^2 above 210 K The corresponding HM values are 0.60 and 0.98, respectively. The whole molecule rotates above 210 K. One of the surprising conclusions is that methyl groups are in a motional state at 2 K.

For the compounds 1,4-dicyclohexylcyclohexane,[25] cyclohexane[26] and adamantane (Bokor, M. et al., to be published), the results are summarized in **Table 2**. Isotropic (not uniaxial) rotation exists in the high symmetry cyclohexane and adamantane molecules in the solid phase.

The results for a few amino acids are also shown in **Table 3**. Amino acids are in zwitterionic form in the crystalline state. Rapid random reorientation of the $-NH_3$ and the $-CH_3$ groups in the solid amino acids were found above 150 K.[35,36] There are two motional processes manifesting themselves in the narrowing of the NMR spectra with increasing temperature. The second moments fall in two successive steps with temperature as the frequency of motion of each process becomes comparable with the spectral width.

A few generalizations are already apparent upon analyzing and comparing data on these organic compounds. Each molecule shows extensive internal mobility in the solid phase at room temperature. In many instances, the mobility of the H-H vectors can be as high as resulting in $HM = 0.95$. The mobile state exists also at lower temperatures, even at $T = 4$ K in some cases. The HM order parameter for the hydrogen mobility is a quantitative measure of the dynamic state, and it requires no model to be applied, in contrast with the second moment measured at a given temperature.

Wide-Line NMR Spectra and Second Moments of Proteins

Studies on small organic molecules and amino acids suggest that the order parameter introduced adequately captures the extent of hydrogen mobility, without invoking a model for interpreting experimental observations. Diakova et al.[37] studied the wide-line ^{1}H-NMR FID signals of dry and hydrated lysozyme powders. The FID of the hydrated protein powder was fitted to a sum of Gaussian functions (plus a constant at the highest water contents). It was found that the residual water at levels below 5 wt% is not rotationally mobile and the water-proton NMR signal is indistinguishable from the FID of the solid protein protons. The fast component of the FID was isolated and analyzed, which corresponds to the majority of the protein protons that do not experience significant dynamical averaging. These experiments infer that our approach might also be used for characterizing the general structural behavior of proteins.

To this end, we selected proteins that fall into two broad structural classes, ordered (folded) and intrinsically disordered

Table 3. Second moments and hydrogen mobility for selected amino acids

	M_2 [10^{-8} T^2]	M_2 [10^{-8} T^2]	M_2 [10^{-8} T^2]	HM
	$T = 4.2$ K	$T = 77$ K	room temp.	(Eq. 5)
glycine		30.3	12.7	0.58
α-alanine		31.8	9.2	0.71
β-alanine		34.9	15.0	0.57
isoleucine	30		11	0.66
leucine	26		8	0.74
methionine	21		nd	nd
threonine	27.5		11.5	0.59
valine	26		11	0.67

(ID or ID protein, IDP), anticipating that IDPs show much more hydrogen mobility and much less order than folded ones. As a representative of ordered proteins, we chose lysozyme, the enzyme that has been amply studied for its structure, function and disease-causing mutations.[38] We then extended our studies on several IDPs which have already been characterized in much detail. Thymosin β4 is a small actin-regulatory protein, which has been shown experimentally to be highly disordered (Á. Tantos, et al., to be published[39]). α-synuclein is also a fully disordered protein,[40,41] involved in Parkinson disease where it undergoes a transition to a highly structured amyloid state. Familial mutations (A30P, E46K, and A53T) promote this transition, possibly via altering the conformational equilibrium and structural flexibility of the protein.[40,41] ERD14 is a plant IDP of stress-related functions,[42,43] also shown to be highly disordered. Our goal here is to characterize these proteins in detail to determine their HM and correlate their behavior with their physiological function and relationship with disease. It is to be noted that some of our conclusions rely on preliminary results, and further experimental results we intend to publish in later detailed publications.

Methods Applied

The applied NMR measurement and evaluation methods were summarized in chapter 13 of reference 10. In addition to the generally used FID signals, solid-echo signals were also detected. Results for the entire temperature range covered (extended down to 4.2 K) are discussed in separate publications. The NMR signals detected in the time domain were analyzed and transformed to spectra similarly as it was described in reference 44.

^{1}H NMR measurements and data acquisition were accomplished by Bruker AVANCE III and Bruker SXP 4–100 NMR pulse spectrometers at $\omega_0/2\pi = 82.4$ MHz with a stability better

Table 4. The results on a polycrystalline globular and a few lyophilized powdered ID proteins.

	Lysozyme	α-synuclein variants				ERD14	Tβ4
		A30P	E46K	WT	A53T		
M_2(He)	16.1	22.2	21.7	17.9 (22.0)	17.2 (22.0)	20.1	22.0
M_2^t(RT)	10.4	8.2	7.8	6.7 (8.6)	8.6 (8.6)	7.6	6.0
M_2^b(RT)	11.0	10.7	9.4	8.9 (11.0)	10.1 (10.1)	10.4	6.8
M_2^n(RT)	0.9	1.7	0.2	0.4	0.4	0.50	0.9
HM^t	0.35	0.63	0.64	0.53 (0.72)	0.50 (0.72)	0.62	0.73
HM^b	0.32	0.52	0.57	0.50 (0.50)	0.41 (0.54)	0.48	0.69
HM^n	0.94	0.92	0.99	0.98	0.98	0.98	0.96

The parameter values in parentheses are given for a hypothetical rigid lattice state. The second moment (M_2) values are given in 10^{-8} T^2 = 1 G^2 units, for the HM^x parameters are defined by Equation 6. The designations He and RT mean $T \sim 4$ K (liquid helium temperature) and room temperature, respectively. The index t refers to the whole spectrum, b stands for the broad while and n for the narrow spectrum component.

than $\pm 10^{-6}$, and with 2 ppm inhomogeneity of the magnet. The temperature was controlled by an open-cycle Janis cryostat with a stability of ± 0.1°C, the uncertainty of the temperature scale was ± 1°C. The data points in the figures are based on spectra recorded by averaging signals to reach the signal/noise ratio 50. The number of averaged NMR signals was varied to achieve the desired signal quality for each sample.

Results and Discussion

The presented NMR-signals are limited to the lowest temperature of 4.2 K and to room temperature. The proteins lysozyme (T. Verebélyi, et al., to be published) and thymosin β$_4$ were chosen as examples representing the expected lowest and highest HM values. The spectra of the FID and the solid-echo signals differ only slightly from each other. The spectrum of the FID is somewhat wider as a consequence of the local magnetic fields coming from inhomogeneous proton-proton contributions. Unlike to the data reported earlier,[37] the shape of the spectrum was not Gaussian either at T = 4.2 K or at room temperature (**Figs. 1–4**). The spectra could be decomposed into at least two components at both low and high temperatures. The presence of different spectral components indicates the heterogeneity of the proton spin-systems. The relative weights of the components vary with the protein types and the temperatures. The room-temperature narrow-spectrum component was wider than a signal coming from "free" water alone. The other proteins listed in **Table 4** show similar behaviors.

The second moments calculated from the spectra and the HM hydrogen mobility parameters are summarized in **Table 4**; one should remember that the t-indexed parameters apply to whole molecules and indices b and n refer to the two-component resolutions. The two-component spectra and the relevant moments measured at room temperature indicate two types of hydrogen-hydrogen radial vector mobility, characteristic of two individual populations of residues of the molecule. The difference between the very-low-temperature second moment M_2^t (He) and the room-temperature second moment of the broad component M_2^b (RT) shows that the molecule has no part made up entirely of static hydrogen atoms (immobile proton-proton radial vectors) at elevated temperatures. Even in the solid phase, the

mobility $HM^t(T)$ characteristic of the whole molecule is considerably greater for the IDP molecules than for globular lysozyme. In accord, the value of $HM^t(T)$ is presumably in close association with structural disorder of proteins. It is of note that these types of molecular motions do not become frozen in aqueous solutions either. The second moments measured for the protein lysozyme at low and high temperatures (M_2^t (He) and M_2 (RT), respectively) give the smallest HM^t value, which we use as a reference point for globular (structured) proteins. Thymosin β$_4$ represents the other extremity, which shows the highest proton-proton radial vector mobility. All the experimental data measured by different methods proves the substantial disorder of the molecule. ERD14 also has a high mobility, which is in line with its largely disordered character as a molecular chaperone.

The results on α-synuclein mutants are important from another point of view. HM provides a qualitative measure of distinction, it is model-free and quantitative, which can be related to the function of IDPs. Whereas it is premature to draw general conclusions, this perfectly fits into the current trend of linking quantitative description structural features of IDPs with their function (unstructure-function relationship), it is of further note that proton-proton mobility of α-synuclein point mutants already shows significant differences at the temperature of liquid helium in the case of WT and A53T, in contrast with E46K and A30P. The smaller M_2^t (He) values for the α-synuclein variants wild-type (WT) and A53T (compared with the two other mutants) can only be explained by assuming that the molecule is not totally rigid even at such low temperatures and they show a mobility of $HM^t \sim 0.20$. It was presumed that the rigid-lattice second moments of the WT and the other α-synuclein mutants are the same with the value M_2(He) = 22·10^{-8} T^2 (numbers in parentheses, **Table 4**). This presumption is reasonable as these α-synuclein variants differ from each other in only one amino acid of 141. By the criterion of HM, wild-type and A53T are the most disordered of the four α-synuclein variants, i.e., they have the most dynamic molecular groups (hydrogen atoms). It is of note that earlier NMR data showed a similar behavior on their frozen aqueous solutions,[41] and these differences in behavior seem to have bearing on the effect of familial mutations on local ordering being conducive to their transition to the disease-related amyloid state.
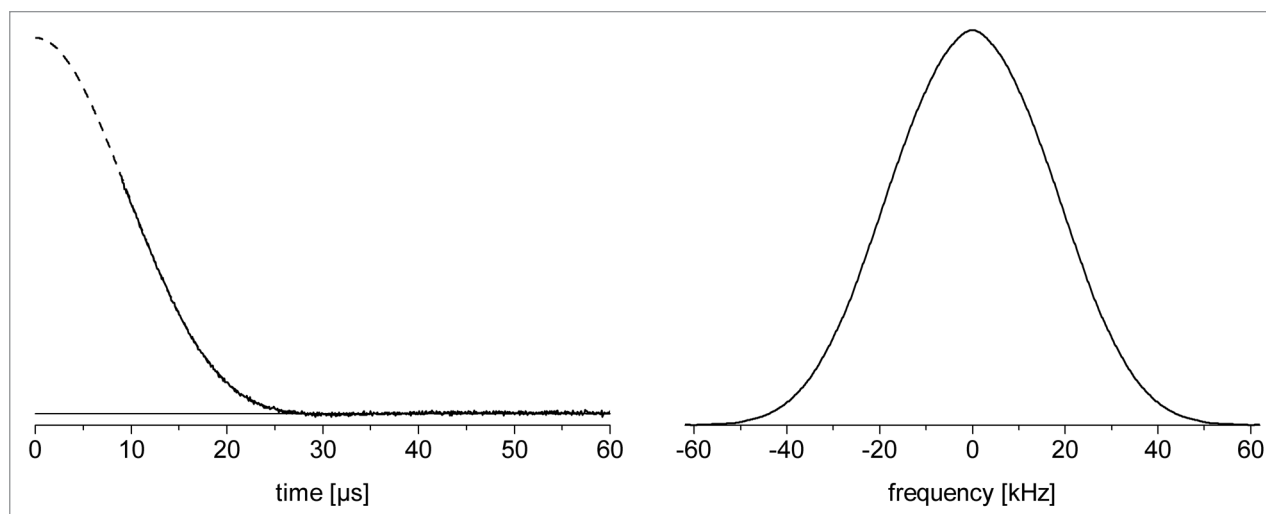
Figure 1. ^{1}H NMR FID (*left*) and spectrum (*right*) of lyophilized lysozyme measured at T = 4.2 K, ν_0 = 82.4 MHz. The spectrum is 41.9 ± 0.2 kHz wide. The second moment (M_2) of the spectrum is (16.1 ± 0.1)·10^{-8} T^2, the fourth moment is M_4 = (87 ± 8)·10^{-17} T^4. The shape factor of the spectrum is M_2^2/M_4 = 3.3 ± 0.3 (it is 3 for a Gaussian). Estimated errors are given.
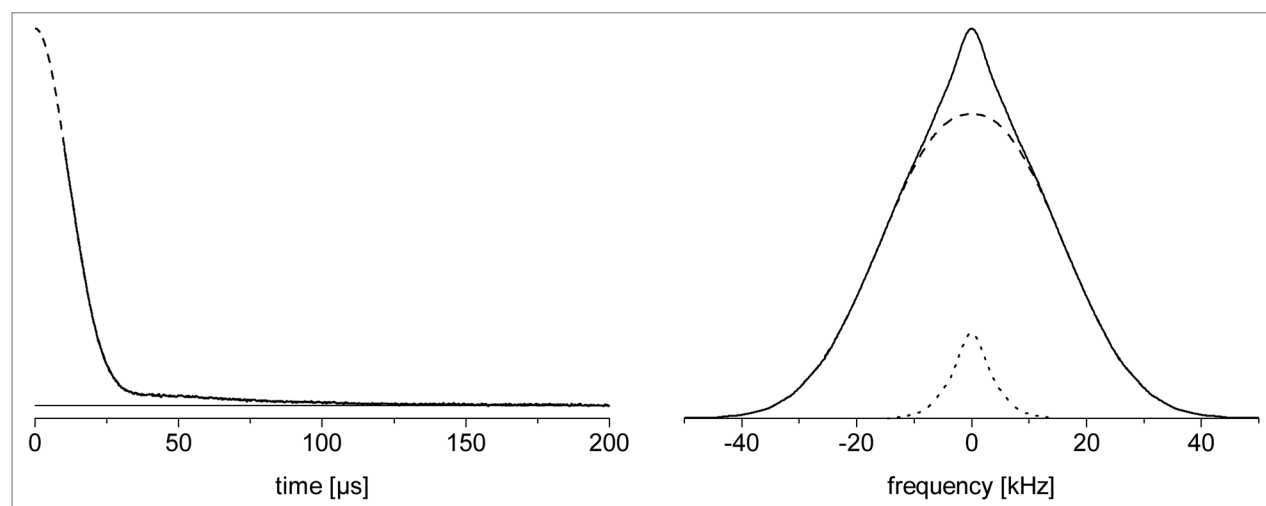
Figure 2. ^{1}H NMR FID (*left*) and spectrum (*right*) of lyophilized lysozyme measured at T = 295.1 K, ν_0 = 82.4 MHz. The spectrum was decomposed into a broad rigid lattice line and a motionally narrowed line. The FID shows fast rigid lattice and slow motionally narrowed relaxation accordingly. The second moment (M_2) of the spectrum is (10.4 ± 0.1)·10^{-8} T^2, the broad line is of M_2 = (11.0 ± 0.1)·10^{-8} T^2 while the narrow line has M_2 = (0.9 ± 0.1)·10^{-8} T^2. The spectral widths are 29.1 ± 0.1 kHz, 35.3 ± 0.2 kHz, and 7.1 ± 0.1 kHz, respectively. (The corresponding shape parameters are 3.50 ± 0.3, 3.32 ± 0.3, and 3.51 ± 0.3, respectively.) Estimated errors are given.

Conclusions and Outlook

The hydrogen mobility order parameter $HM(T)$ proposed here represents the relative missing part of the time-independent (rigid lattice) ^{1}H NMR second moment coming from the proton-proton dipole-dipole interaction in hydrogen rich molecules, including organic compounds, amino acids and proteins. HM can take values between 0 and 1, characteristic of a rigid lattice and liquid state, respectively, and the actual values are temperature dependent quantities.

In the context of the present study, the term motion is needed for the internal motions of a molecule (not for the translational diffusion of molecules in a liquid), and the time scale is set by the motions visible to NMR. The above results together with the introduction of the order parameter represent a theoretical and practical framework that can guide further investigations and assist in classifying proteins.

It is worthy to address why we chose the order parameter and not the second moment to characterize mobility? To calculate the second moment of a rigid lattice, precise atomic coordinates are needed, which can be obtained only by applying models. In the case of active molecular motions, the details of these motions should also be modeled. It is fair to ask how many parameters should be introduced to interpret a single measured quantity. Molecular motions result in almost twice as many parameters than a rigid system. The hydrogen mobility introduced here
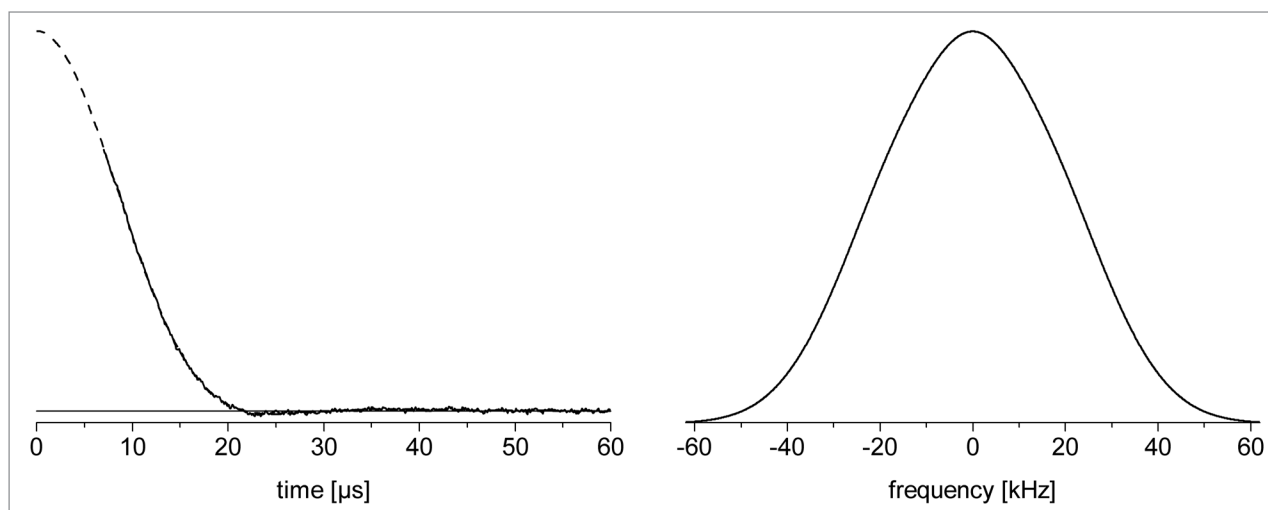
Figure 3. ^{1}H NMR FID (*left*) and spectrum (*right*) of lyophilized Tβ4 measured at T = 7.4 K, ν_0 = 82.4 MHz. The spectrum is 49.5 ± 0.2 kHz wide. The second moment (M_2) of the spectrum is (20.6 ± 0.1)·10^{-8} T^2, the fourth moment is M_4 = (117 ± 10)·10^{-17} T^4. The shape factor of the spectrum is M_2^2/M_4 = 2.7 ± 0.3 (it is 3 for a Gaussian). Estimated errors are given.
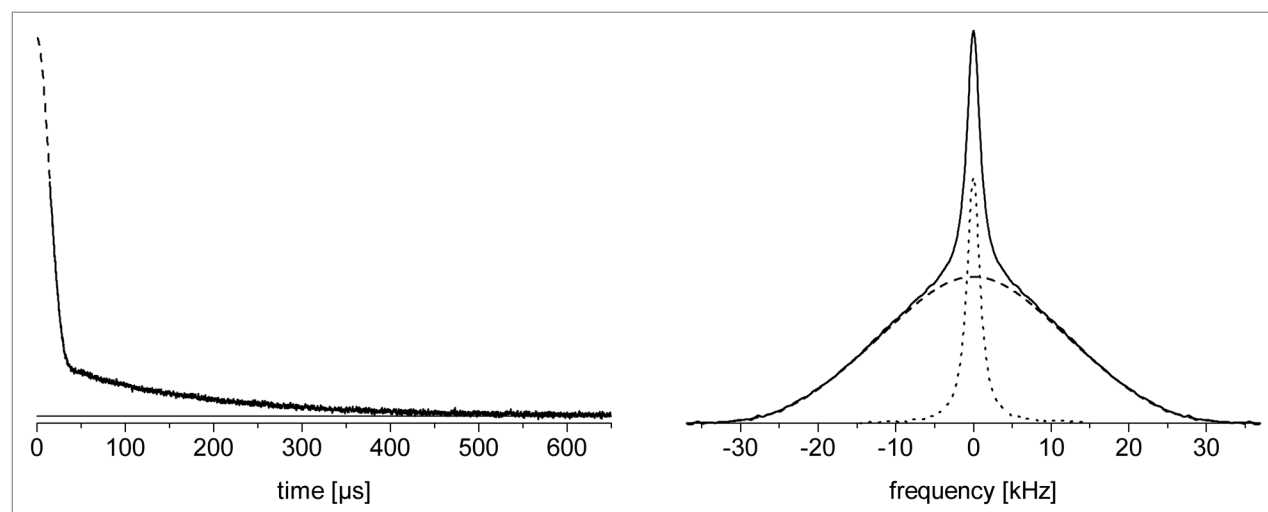
Figure 4. ^{1}H NMR FID (*left*) and spectrum (*right*) of lyophilized Tβ4 measured at T = 300 K, ν_0 = 82.4 MHz. The spectrum was decomposed into a broad rigid lattice line and a narrow motionally narrowed line. The FID shows fast rigid lattice and slow motionally narrowed relaxation accordingly. The second moment (M_2) of the spectrum is (6.2 ± 0.1)·10^{-8} T^2, the broad line is of M_2 = (7.0 ± 0.1)·10^{-8} T^2 while the narrow line has M_2 = (0.5 ± 0.1)·10^{-8} T^2. The spectral widths are 3.8 ± 0.1 kHz, 27.9 ± 0.1 kHz, and 0.5 ± 0.05 kHz, respectively. (The corresponding shape parameters are 3.8 ± 0.3, 3.0 ± 0.3, and 11.2 ± 0.3, respectively.) Estimated errors are given.

provides an overall dynamic attribute, i.e., a model-independent quantitative value, which characterizes the general internal dynamics of the molecule at the actual temperature. It is hard to overemphasize that only two measured quantities are used in the hydrogen mobility factor, namely the reduced second moment measured at the actual temperature and a reference second moment value measured for the rigid-lattice state. It is not at all intended to exclude models as tools to help the interpretation of the measured second moments. For example, the four variants of α-synuclein have almost identical primary structures, yet their NMR spectra and second moments show explicit differences even at T < 10 K.

The knowledge of the measured M_2(RL) gives significant help in explaining the NMR relaxation times. The coupling constant of the relaxation formalisms (see e.g., Chapter 12 in ref. 9, and Chapter 13 in refs. 10,15, and 45) can be determined directly from the second moment of the rigid lattice. Therefore, not all three of the quantities—coupling constant, activation energy, and correlation time—only the latter two, should be determined from the relaxation time vs. temperature curves. We previously found that the three-parameter fitting of the relaxation time model produces absurd results in the case of the IDPs.[46] The spatial and the temporal averages are immiscible categories for heterogeneous systems such as the protein molecules.

Our results prove that the proposed order parameter (*HM*) for hydrogen mobility is a well-defined physical quantity, which can be experimentally determined in a model-free way for small molecules and proteins alike. Furthermore, it does not involve any speculation or reference to "fitting parameters". *HM* provides a theoretical and practical framework for the investigation of the correlations between global structural order and internal molecular mobility in solids. It provides a simple yet powerful method for the fast and quantitative distinction between globular and ID proteins. Whereas order parameters of individual resonances have the power of resolving detailed structural features of proteins (globular and ID alike), there is a strong trend in the IDP literature that uses global parameters of structure, disorder, and flexibility for approaching their function. In this sense, the novel parameter fits into the general characterization of IDPs. It even has the power to show quantitative differences between the dynamics of proteins, the sequence of which differ only in one amino acid. It provides a bridge connecting the dynamic properties measured for aqueous solutions and lyophilized proteins. And finally, *HM* calls attention to the importance of precise measurements and the adequate selection of reference temperatures.

References

1. Halle B. Protein hydration dynamics in solutions, Phyl. Trans. R Soc Lond B 2004; 359:1207-24; http://dx.doi.org/10.1098/rstb.2004.1499

2. Saito N, Kobayashi Y. 2001. The physical foundation of protein architecture. World Scientific Publishing Company, Singapore, New Jersey, London, Hong Kong.

3. Wlodawer A, Minor W, Dauter Z, Jaskolski M. Protein crystallography for non-crystallographers, or how to get the best (but not more) from published macromolecular structures. FEBS J 2008; 275:1-21; PMID:18034855; http://dx.doi.org/10.1111/j.1742-4658.2007.06178.x

4. Dyson HJ, Wright PE. Unfolded proteins and protein folding studied by NMR. Chem Rev 2004; 104:3607-22; PMID:15303830; http://dx.doi.org/10.1021/cr030403s

5. Duer MJ. 2007. NMR Techniques for Studying Molecular Motion in Solids. In Solid-State NMR Spectroscopy Principles and Applications. M. J. Duer editor. Blackwell Science Ltd, Oxford, UK.

6. Antzutkin ON. 2007. Molecular Structure Determination: Applications in Biology. In Solid-State NMR Spectroscopy Principles and Applications. M. J. Duer editor. Blackwell Science Ltd, Oxford, UK.

7. Smith GM. 1995. Studies of Protein Structure by NMR Spectroscopy. In Annual Reports on NMR Spectroscopy. G. A. Webb, P. S. Belton, M. J. McCarthy, editors. Academic Press, London. 31:171-218.

8. Tompa P. 2009. Structure and Function of Intrinsically Disordered Proteins. Chapman and Hall/CRC, University of Cambridge, UK.

9. Uversky VN, Longhi S, eds. 2010. Instrumental Analysis of Intrinsically Disordered Proteins: Assessing Structure and Conformation. John Wiley & Sons, Inc., Hoboken, NJ, USA.

10. Uversky VN, Dunker AK, eds. 2012. Intrinsically Disordered Protein Analysis. Vol. 1, Methods and Experimental Tools. Vol.1. Springer Protocols. Humana Press, Springer, New York.

11. Mansfield P. 1971. Pulsed NMR in Solids. In Progress in Nuclear Magnetic Resonance Spectroscopy, Vol 8. Issue 1. J. W. Emsley, J. Feeney, L. H, Sutcliffe, editors. Pergamon Press, Oxford. 43-101.

12. McBrierty VJ, Packer KJ. 1993. Nuclear magnetic resonance in solid polymers. Cambridge University Press, Cambridge UK.

13. Van Vleck JH. The dipolar broadening of magnetic resonance lines in crystals. Phys Rev 1948; 74:1168-83; http://dx.doi.org/10.1103/PhysRev.74.1168

14. Abragam A. 1961. The principles of nuclear magnetism. Oxford University Press, London.

15. Slichter CP. 1990. Principles of Magnetic Resonance. Springer Verlag, Third Edition, Berlin, Heidelberg.

16. Andrew ER, Eades RG. A Nuclear Magnetic Resonance Investigation of Three Solid Benzenes. Proc Roy Soc A 1953; 218:537-52; http://dx.doi.org/10.1098/rspa.1953.0123

17. Andrew ER. 1971. The narrowing of NMR spectra of solids by high-speed specimen rotation and the resolution of chemical shift and spin multiplet structures for solids. In Progress in Nuclear Magnetic Resonance Spectroscopy, Vol 8. Issue 1. J. W. Emsley, J. Feeney, L. H, Sutcliffe, editors. Pergamon Press, Oxford. 1-39.

18. Goc R. Simulation of the NMR Second Moment as a Function of Temperature in the Presence of Molecular Motion. Application to $(CH_3)_3NBH_3$. Z Naturforschung. 2002; 57A:29-35

19. Kittel C, Kroemer H. 1980. Thermal Physics. W.H. Freeman and Company, San Francisco.

20. Landau LD, Lifshitz EM. 1980. Statistical Physics, Third Edition, Part 1: Volume 5 (Course of Theoretical Physics, Volume 5). E. M. Lifshitz and L. P. Pitaevskii, editors. Part 1, Discussion of many topics of interest to physicists. Pergamon, Elmsford, NY.

21. Priestley EB, Wojtowitz PJ. Ping Sheng Eds. 1974. Introduction to Liquid Crystals. Plenum Press, New York and London, Chs 3. and 6.

22. Pake GE. Nuclear Resonance Absorption in Hydrated Crystals: Fine Structure of the Proton Line. J Chem Phys 1948; 16:327-36; http://dx.doi.org/10.1063/1.1746878

23. Porte AL, Gutowsky HS, Harris GM. Proton Magnetic Resonance Study of Crystalline Potassium Trisoxalatorhodium(III). Hydrate J Chem Phys 1961; 34:66-71; http://dx.doi.org/10.1063/1.1731617

24. Porte AL, Gutowsky HS, Boggs JE. Proton Magnetic Resonance Studies of Polycrystalline Uranium Oxide Hydrate II.β-UO_3H_2O. J Chem Phys 1962; 36:1700-3; http://dx.doi.org/10.1063/1.1701254

25. Andrew ER. Molecular Motion in Certain Solid Hydrocarbons. J Chem Phys 1950; 18:607-18; http://dx.doi.org/10.1063/1.1747709

26. Grüner. Gy. and K. Tompa. 1968. Molekuláris mozgások vizsgálata szilárdtestekben NMR módszerrel. Kémiai kozlemények: a Magyar Tudományos Akadémia Kémiai Tudományok Osztályának kozleményei. 30:315-356. (Study of molecular motions in solids by NMR method. In Chemical communications of the Chemical Sciences Department, Hungarian Academy of Sciences).

27. Andrew ER. R.G. Eades A Nuclear Magnetic Resonance Investigation of Three Solid Benzenes. Proc Roy Soc 1953; A218:537-52

28. Müller A. A Further X-Ray Investigation of Long Chain Compounds (n-Hydrocarbon). Proc R Soc Lond, A Contain Pap Math Phys Character 1928; 120:437-59; http://dx.doi.org/10.1098/rspa.1928.0158

29. Müller A. The Crystal Structure of the Normal Paraffins at Temperatures Ranging from that of Liquid Air to the Melting Points. Proc R Soc Lond, A Contain Pap Math Phys Character 1930; 127:417-30; http://dx.doi.org/10.1098/rspa.1930.0068

30. Müller A. An X-Ray Investigation of Normal Paraffins Near Their Melting Points. Proc R Soc Lond, A Contain Pap Math Phys Character 1932; 138:514-30; http://dx.doi.org/10.1098/rspa.1932.0200

31. Tompa K, Tóth F. 1966. Szilárd dimetilanilin fizikokémiai vizsgálata 2. Proton mágneses rezonancia spektrum. KFKI közlemények Vol. 14, No. 5. (Proton magnetic resonance study of solid dimethylaniline. In Reports of the Central Research Institute for Physics, Hungarian Academy of Sciences).

32. Kromhout RA, Moulton WG. Nuclear Magnetic Resonance: Structure of the Amino Group I. J Chem Phys 1955; 23:1673-9; http://dx.doi.org/10.1063/1.1742408

33. Allen PS, Cowking A. Nuclear Magnetic Resonance Study of Hindered Rotations in Some Methylbenzenes. J Chem Phys 1968; 49:789-97; http://dx.doi.org/10.1063/1.1670141

34. Allen PS, Cowking A. Nuclear Magnetic Resonance Study of Molecular Motions in Hexamethylbenzene. J Chem Phys 1967; 47:4286-9; http://dx.doi.org/10.1063/1.1701629

35. Andrew ER, Hinshaw WS, Hutchins MG, Sjöblom ROI. Proton magnetic relaxation and molecular motion in polycrystalline amino acids. I. Aspartic acid, cysteine, glycine, histidine, serine, tryptophan and tyrosine. Mol Phys 1976; 31:1479-88; http://dx.doi.org/10.1080/00268977600101151

36. Andrew ER, Hinshaw WS, Hutchins MG, Sjöblom ROI. Proton magnetic relaxation and molecular motion in polycrystalline amino acids. II. Alanine, isoleucine, leucine, methionine, norleucine, threonine and valine. Mol Phys 1976; 32:795-806; http://dx.doi.org/10.1080/00268977600102231

37. Diakova G, Goddard YA, Korb J-P, Bryant RG. Changes in protein structure and dynamics as a function of hydration from ^{1}H second moments. J Magn Reson 2007; 189:166-72; PMID:17920315; http://dx.doi.org/10.1016/j.jmr.2007.09.005

38. Booth DR, Sunde M, Bellotti V, Robinson CV, Hutchinson WL, Fraser PE, Hawkins PN, Dobson CM, Radford SE, Blake CC, et al. Instability, unfolding and aggregation of human lysozyme variants underlying amyloid fibrillogenesis. Nature 1997; 385:787-93; PMID:9039909; http://dx.doi.org/10.1038/385787a0

39. Domanski M, Hertzog M, Coutant J, Gutsche-Perelroizen I, Bontems F, Carlier MF, Guittet E, van Heijenoort C. Coupling of folding and binding of thymosin beta4 upon interaction with monomeric actin monitored by nuclear magnetic resonance. J Biol Chem 2004; 279:23637-45; PMID:15039431; http://dx.doi.org/10.1074/jbc.M311413200

40. Bussell R Jr., Eliezer D. Residual structure and dynamics in Parkinson's disease-associated mutants of alpha-synuclein. J Biol Chem 2001; 276:45996-6003; PMID:11590151; http://dx.doi.org/10.1074/jbc.M106777200

41. Házy E, Bokor M, Kalmar L, Gelencser A, Kamasa P, Han K-H, Tompa K, Tompa P. Distinct hydration properties of wild-type and familial point mutant A53T of α-synuclein associated with Parkinson's disease. Biophys J 2011; 101:2260-6; PMID:22067166; http://dx.doi.org/10.1016/j.bpj.2011.08.052

42. Kovacs D, Kalmar E, Torok Z, Tompa P. Chaperone activity of ERD10 and ERD14, two disordered stress-related plant proteins. Plant Physiol 2008; 147:381-90; PMID:18359842; http://dx.doi.org/10.1104/pp.108.118208

43. Szalainé Ágoston B, Kovács D, Tompa P, Perczel A. Full backbone assignment and dynamics of the intrinsically disordered dehydrin ERD14. Biomol NMR Assign 2011; 5:189-93; PMID:21336827; http://dx.doi.org/10.1007/s12104-011-9297-2

44. Derbyshire W, Van Den Bosch M, Van Dusschoten D, MacNaughtan W, Farhat IA, Hemminga MA, Mitchell JR. Fitting of the beat pattern observed in NMR free-induction decay signals of concentrated carbohydrate-water solutions. J Magn Reson 2004; 168:278-83; PMID:15140438; http://dx.doi.org/10.1016/j.jmr.2004.03.013

45. Noack F. 1971. Nuclear Magnetic Relaxation Spectroscopy. In NMR Basic principles and progress. Vol. 3. P. Diehl, E. Fluck, and R. Kosfeld, editors. Sringer-Verlag, Berlin-Heidelberg-New York. pp. 83-144.

46. Bokor M, Csizmók V, Kovács D, Bánki P, Friedrich P, Tompa P, Tompa K. NMR relaxation studies on the hydrate layer of intrinsically unstructured proteins. Biophys J 2005; 88:2030-7; PMID:15613629; http://dx.doi.org/10.1529/biophysj.104.051912

47. Powles JG, Carazza B. 1970. An information theory of line shape in nuclear magnetic resonance. In Magnetic resonance. Proceedings of the International Symposium on Electron and Nuclear Magnetic Resonance, held in Melbourne, August 1969, sponsored by the Australian Academy of Science. C. K. Coogan, N. S. Ham, S. N. Stuart, J. R. Pilbrow, G. V. H. Wilson, editors. Plenum Press New York. pp. 133-161.

48. Lipari G, Szabo A. Model-free approach to the interpretation of nuclear magnetic resonance relaxation in macromolecules. 1. Theory and range of validity. J Am Chem Soc 1982; 104:4546-59; http://dx.doi.org/10.1021/ja00381a009

49. Lipari G, Szabo A. Model-free approach to the interpretation of nuclear magnetic resonance relaxation in macromolecules. 2. Analysis of experimental results. J Am Chem Soc 1982; 104:4559-70; http://dx.doi.org/10.1021/ja00381a010

50. Bertini I, Gupta YK, Luchinat C, Parigi G, Schlörb C, Schwalbe H. NMR spectroscopic detection of protein protons and longitudinal relaxation rates between 0.01 and 50 MHz. Angew Chem Int Ed Engl 2005; 44:2223-5; PMID:15751103; http://dx.doi.org/10.1002/anie.200462344

51. Andrec M, Montelione GT, Levy RM. Estimation of dynamic parameters from NMR relaxation data using the Lipari-Szabo model-free approach and Bayesian statistical methods. J Magn Reson 1999; 139:408-21; PMID:10423379; http://dx.doi.org/10.1006/jmre.1999.1839

Appendices

Appendix A

Thermal energy in a solid can produce motions ranging from lattice vibrations to restricted rotations of parts or the whole of molecules and even translational diffusion. The effect they produce depends on their frequency spectrum, spatial amplitude and the relationship of the motional axes with respect to those defining nuclear spin interactions. When motional averaging is present, the effective interaction which contributes to the spectral shape and width is the average over this motion.[12]

Appendix B

Moment is a quantity that expresses the average or expected value of the first, second, third, or fourth power of the deviation of each component of a frequency distribution from some given value, typically mean or zero. The first moment is the mean, the second moment the variance, the third moment the skew, and the fourth moment the kurtosis. The dipolar interaction between protons gives symmetrical wide-line NMR spectra and consequently zero odd and non-zero even moments. The detailed information theory of the NMR line shape and moments are given in the work of Powles and Carazza.[47]

Appendix C

For fast internal motions of proteins, the (generalized, or effective, or rigidity, or mobility) order parameter S[48,49] is used in the literature (see also e.g., refs. 50 and 51), which is the measure of the degree of spatial restriction of the motion. These order parameters meet a persistent and common claim and have the following common properties. (1) They are used for the interpretation of the relaxation characteristics (R_1, R_2, NMRD, correlation function) measured for aqueous protein solutions and not for solid state proteins as in the examples analyzed here by us. (2) The mathematical relations, which describe the above relaxation characteristics, were determined relying upon multi-parameter fittings. (3) That is, we think that it is not expedient to make a comparison between the order parameters S and HM, in the absence of a critical review on the whole field (and before additional measurements of HM for several more proteins).